LASER INTERFEROMETER GRAVITATIONAL WAVE OBSERVATORY
- LIGO -
CALIFORNIA INSTITUTE OF TECHNOLOGY
MASSACHUSETTS INSTITUTE OF TECHNOLOGY

Engineering Note	**LIGO-E1500247–v1**	2015/07/23

LIGO SURF Progress Report 1: Investigation of Thermal Noise in Thin Silicon Structures

Matthew Winchester
Mentors: Nicolas Smith, Zach Korth, Rana Adhikari

California Institute of Technology
LIGO Project, MS 18-34
Pasadena, CA 91125
Phone (626) 395-2129
Fax (626) 304-9834
E-mail: info@ligo.caltech.edu

Massachusetts Institute of Technology
LIGO Project, Room NW22-295
Cambridge, MA 02139
Phone (617) 253-4824
Fax (617) 253-7014
E-mail: info@ligo.mit.edu

LIGO Hanford Observatory
Route 10, Mile Marker 2
Richland, WA 99352
Phone (509) 372-8106
Fax (509) 372-8137
E-mail: info@ligo.caltech.edu

LIGO Livingston Observatory
19100 LIGO Lane
Livingston, LA 70754
Phone (225) 686-3100
Fax (225) 686-7189
E-mail: info@ligo.caltech.edu

http://www.ligo.caltech.edu/

1 Introduction

LIGO (Laser Interferometer Gravitational-Wave Observatory) is a massive physics experiment designed to detect gravitational waves originally predicted by Einstein's general theory of relativity in 1916. Each detector is essentially a Michelson interferometer. As gravitational waves pass through the detectors, they distort local space-time and change the effective path length difference between the two perpendicular arms of the interferometer. This creates a relative phase shift between the two beams and allows for constructive interference at the photodiode detector, resulting in a measureable signal that indicates the presence of gravitational waves. Two independent detectors have been built and operated in Livingston, Louisiana and Hanford, Washington. The second generation of LIGO detectors, Advanced LIGO (aLIGO), have been constructed and are currently being commissioned to optimize sensitivity. The first data run of aLIGO is scheduled to begin in Fall 2015.

Research has already begun concerning the third generation of LIGO detectors. There are many different sources of noise that limit the precision of the experiment, such as shot noise, seismic vibrations, and thermal noise. In the frequency band relevant for the detection of gravitational waves (10-100Hz), thermal noise in the test masses and suspensions is currently a major factor limiting precision. The aLIGO test masses and suspensions are made of a fused silica material. Cryogenic silicon is now being considered as an alternative construction material for the next generation of LIGO detectors in order to further reduce thermal noise and increase sensitivity in the low frequency band of interest [1].

Thermal noise can be very difficult to measure directly. However, the fluctuation-dissipation theorem relates the dissipation of a perturbed system to the thermal fluctuations of the system at equilibrium. This means that the mechanical dissipation of the material can be studied instead, and this is usually a much easier approach in practice. Previous work has been done investigating the quality factor of thin silicon flexures through ringdown measurement techniques [2, 3]. This project focuses on both ringdown measurements and more advanced techniques such as continuous measurements using feedback control loops.

2 Driven, Damped Oscillators

An externally driven oscillator with linear damping is most commonly modeled as the differential equation:

$$m\ddot{x} + b\dot{x} + kx = f_{ext} \tag{1}$$

where m is the mass of the oscillator, b is the damping coefficient, and k is the restorative spring constant. This differential equation is easy to solve in the frequency domain by taking the Laplace transform:

$$ms^2X(s) + bsX(s) + kX(s) = F_{ext}(s) \tag{2}$$

The transfer function of the system is defined as the ratio of $X(s)/F_{ext}(s)$:

$$H(s) = \frac{X(s)}{F_{ext}(s)} = \frac{1}{ms^2 + bs + k} \tag{3}$$

The system acts as a second order low pass filter. Our resonators have very small dissipation, so we focus on the case of underdamped motion, where $b^2/4km \ll 1$. It is also convenient to introduce the three terms $\gamma = b/m$ (damping ratio), $\omega_0 = \sqrt{k/m}$ (natural frequency), and $\tau = 2/\gamma$ (characteristic time). In this regime, the two poles of the transfer function are at:

$$s = \frac{-\gamma}{2} \pm i\sqrt{\omega_0^2 - \gamma^2/4} \tag{4}$$

The maximum value of $|H(i\omega)|$ is at the frequency $\omega_{max} = \sqrt{\omega_0^2 - \gamma^2/2}$. Taking the same underdamped limit above, the γ^2 term is negligible so $\omega_{max} \approx \omega_0$. A plot of the transfer function with normalized frequency is shown in Figure 1 below, with $\gamma = 0.05$:

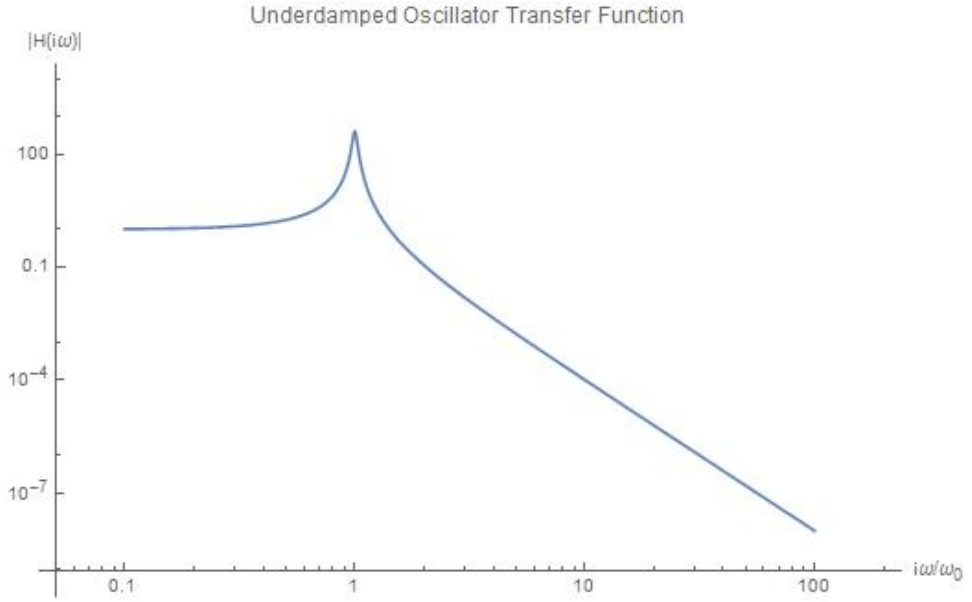

Figure 1: Oscillator Transfer Function

The quality factor Q of the resonator is defined as $Q = \omega_0/\Delta$, where Δ is the full width half max of the transfer function peak. From this definition, we have:

$$Q = \omega_0/\gamma = \frac{\omega_0\tau}{2} \tag{5}$$

The impulse response of the system can be found by taking the inverse Laplace transform of the transfer function:

$$x(t) = e^{-t/\tau}\sin\left(t\sqrt{\omega_0^2 - \gamma^2/4}\right) \tag{6}$$

where again the γ^2 term can be safely ignored, so the final form of the impulse response is:

$$x(t) = e^{-t/\tau}\sin\left(\omega_0 t\right) \tag{7}$$

This is simply a damped sinusoid, and an example trace of an underdamped oscillator is shown below:

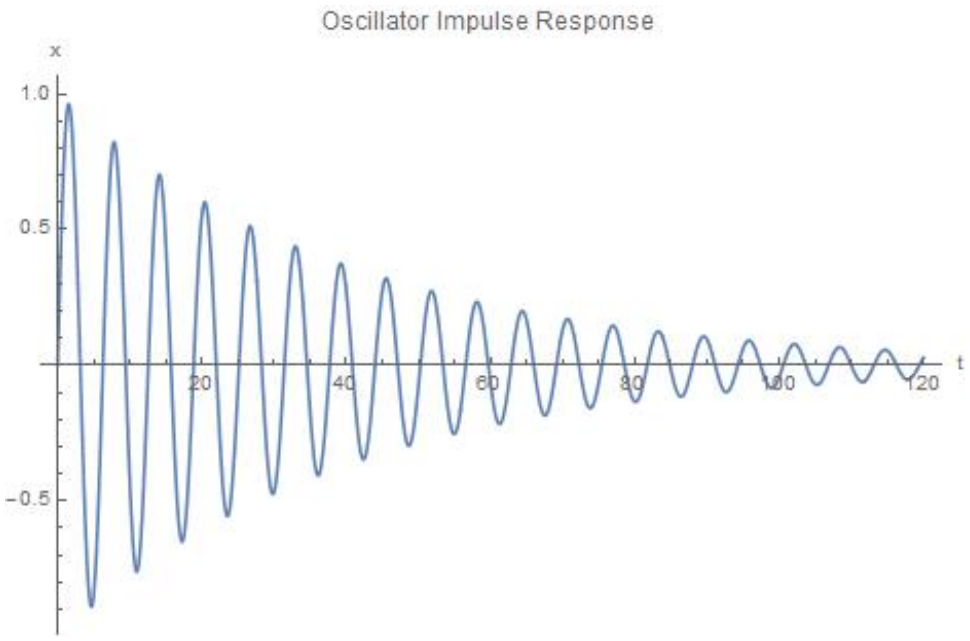

Figure 2: Oscillator Impulse Response

3 Internal Damping

Equation 1 is not the only way to model a damped system. Internal damping within materials is frequently described using a complex spring constant k [4]. In this model, the equation of motion becomes:

$$m\ddot{x} + k(1 + i\phi)x = f_{ext} \tag{8}$$

where $\phi(\omega)$ is called the loss angle. The loss angle represents the phase lag between a sinusoidal restorative force and the resulting sinusoidal displacement. It can be shown that the oscillator loses a fraction $2\pi\phi$ of its kinetic energy per cycle by intergrating the work done by the restorative force over a single displacement period. Again taking the Laplace transform and setting the two different parametrizations equal to each other yields the expression:

$$\gamma(\omega) = \frac{\omega_0^2 \phi}{\omega} \tag{9}$$

The quality factor is only defined on resonance $\omega = \omega_0$, so:

$$Q = \frac{1}{\phi(\omega_0)} = \frac{\omega_0 \tau}{2} \tag{10}$$

This relationship forms the motivation for studying the decay time τ of the oscillator. By measuring τ we can calculate the loss ϕ, which then tells us about the thermal noise of the resonator through the fluctuation-dissipation theorem.

4 Thermoelastic Loss

Mechanical losses in solids come from a variety of different dissipation mechanisms. These include processes such as phonon-phonon loss, surface loss, and bulk loss. We expect thermoelastic loss to be a significant loss mechanism due to our silicon resonator geometry. Thermoelastic loss occurs when a solid is bent. As certain local regions are compressed they heat up, while stretched regions are cooled (assuming a positive coefficient of thermal expansion). This creates temperature gradients in the material. Heat fluxes driven by the temperature gradient irreversibley dissipate energy, thus causing loss. Since thermoelastic loss is highly dependent on the material coefficient of thermal expansion, cryogenic silicon naturally becomes a good material choice for high quality mechanical systems due to its vanishing coefficient of thermal expansion at 124K.

For isotropic materials in pure bending modes, the thermoelastic loss ϕ_{TE} is given by the equation [5]:

$$\phi_{TE} = \frac{\alpha^2 Y T}{\rho C_p} \frac{\omega\tau}{1+\omega^2\tau^2} \tag{11}$$

where α is the coefficient of thermal expansion, Y is Young's modulus, T is the temperature, ρ is the material density, C_p is the heat capacity, and ω is the angular frequency of the particular bending mode. The additional time constant τ is defined as:

$$\tau = \frac{\rho C_p t^2}{\pi\kappa} \tag{12}$$

where t is the thickness of the resonator and κ is the thermal conductivity. Figure 3 below shows several plots of the thermoelastic loss as a function of temperature and angular frequency. A thickness $t = 50\mu m$ is assumed:

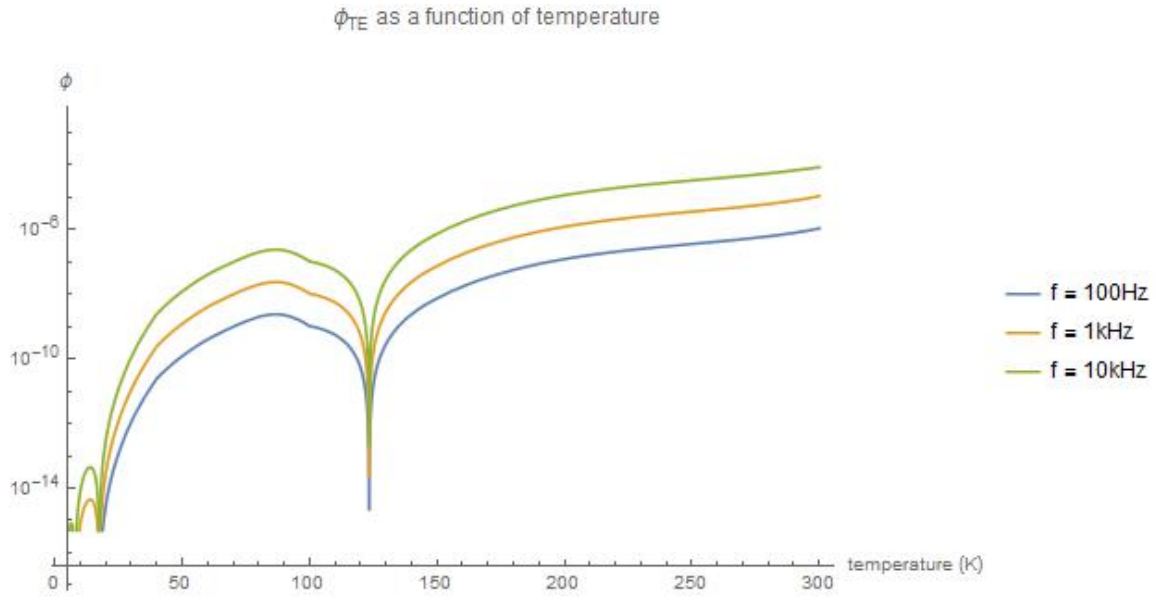

Figure 3: Thermoelastic Loss

5 Ringdown Measurements

In the ringdown experiment we determine the Q factor and loss angle of a thin silicon cantilever by measuring the time constant τ of a damped sinusoidal amplitude signal. The cantilever is mounted on one end using a stainless steel clamp and the other end is driven using an electrostatic driver (ESD). The entire system is tested in a cryostat where is operates in vacuum at cryogenic temperatures using liquid nitrogen to cool the enclosure. The cantilever displacement is measured by sending a HeNe laser beam through a window in the cryostat. After the beam is reflected off of the cantilever, it returns to a calibrated quadrant photodiode which measure the position of the beam which is proportional to the cantilever displacement. Additional components in the system include a power resistor used to control resonator temperature and a PEEK base underneath the clamp for insulation from the cold plate. The (old) experimental setup is shown below:

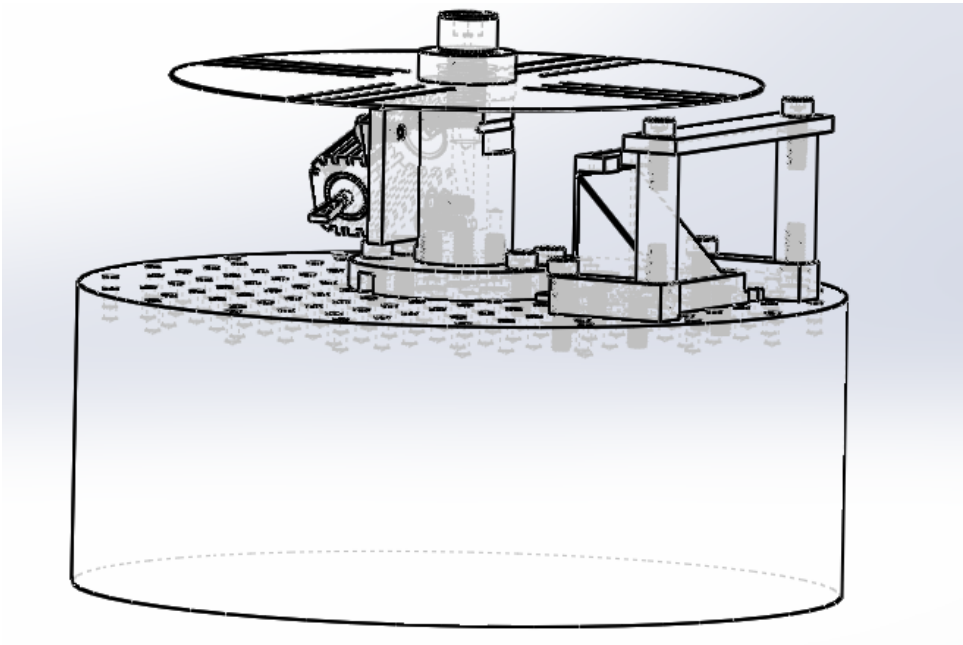

Figure 4: Experimental Assembly

So far we have analyzed two different cantilevers using the ringdown method. The general data analysis procedure consists of taking a fourier transform of the amplitude signal and then bandpass filtering around the resonant frequency of the oscillator. An exponential curve can then be fitted to the filtered time domain signal in order to estimate the decay time τ. Several plots outlining this procedure are shown in Figure 5 below:

In the example analysis below, the Q was determined to be $\approx 28,000$ with $\omega_0/2\pi = 144.6$Hz.

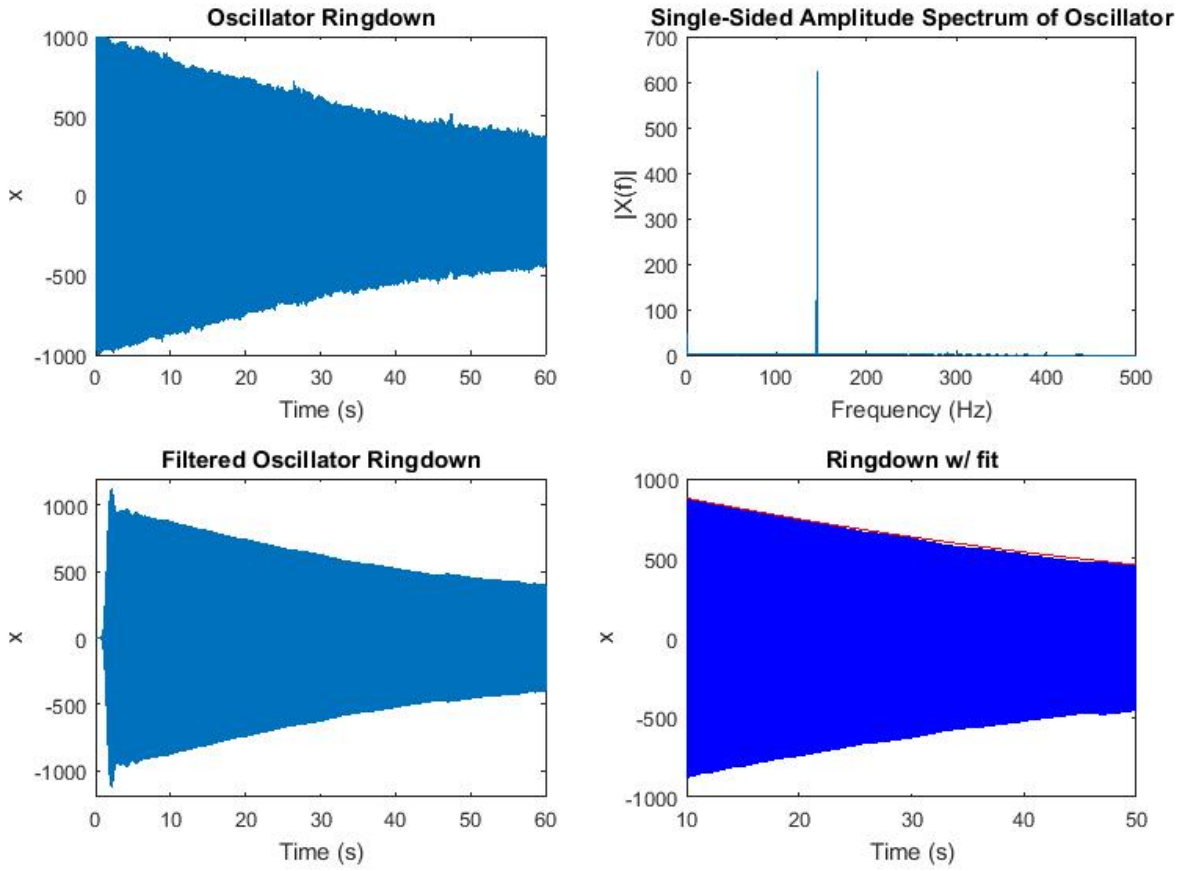

Figure 5: Data Analysis Procedure

6 Clamp Design

We are never truly measuring the cantilever loss in any of our experiments because the cantilever isn't a closed system fixed to an infinitely stiff anchor. Our measured loss is an aggregate of losses in the cantilever, clamp, PEEK base, and even the cyrostat itself. Losses in the clamp have been significant in previous experiments, so optimizing the clamp design to minimize loss is an important task.

A new clamp model was recently designed for the next series of quality factor measurements. Major changes from the previous model include a much thicker diameter and a lip to constrain the sapphire washers and pinwheel cantilever itself in an effort to decrease clamp loss. The design can be seen below:

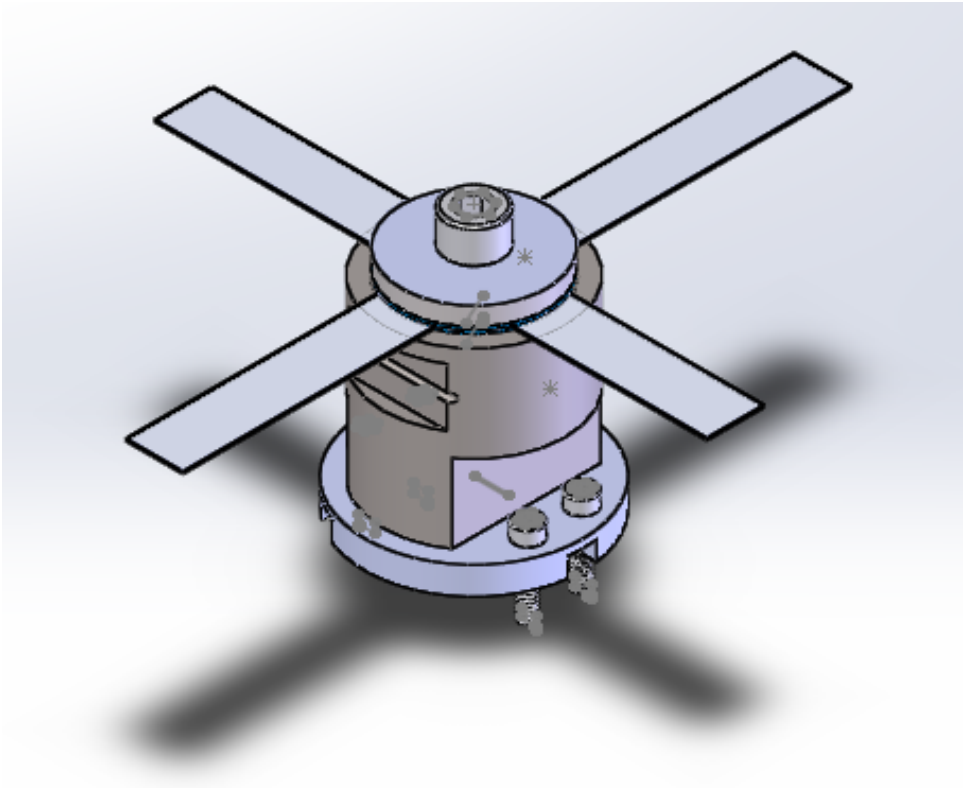

Figure 6: New Clamp Design

7 Future Work

We are going to continue testing different surface treatments and geometries of silicon flexures in order to find the optimal cantilever design. This will involve working with other applied physics groups on campus that have experience with the different surface treatment techniques that we require. Different clamp assemblies may also need to be developed and tested if our measurements still indicate that we are limited by clamp loss. Once we begin to see significant improvements in the quality factor of the resonators, we will begin to measure

loss using more advanced systems such as the continuous measurement method discussed previously.

Finite element analysis techniques through COMSOL may also be used in order to model the loss mechanisms of different silicon cantilever systems. This will involve learning the FEA method and becoming familiar with COMSOL software.

A larger cryogenic experiment is also currently under construction. Once the optimal silicon flexure design has been attained, it will be incorporated into the other experiment. The goal of this larger experiment is to directly measure the thermal noise in thin silicon structures by locking a laser to two separate cavities. Each cavity consists of a static mirror and a mirror attached to a silicon structure. Thermal noise can then be measured interferometrically by looking at the beat note formed by the two locked laser beams. The experiment is well into assembly; most optical and electronic systems have been set up.

References

[1] A.V. Cumming, L. Cunningham, G. D. Hammond, K. Haughian, J. Hough, S. Kroker, I. W. Martin, R. Nawrodt, S. Rowan, C. Schwarz, and A. A. van Veggel, *Silicon mirror suspensions for gravitational wave detectors*. Quantum Grav. 31 025017 (2013).

[2] Edward Taylor, Nicolas Smith, *Quality Factor of Crystalline Silicon at Cryogenic Temperatures*. LIGO Document P1300172-v1 (2013).

[3] Marie Lu, Nicolas Smith, Rana Adhikari, Zach Korth, *Measuring the Quality Factor of Cryogenic Silicon*. LIGO Document T1400668-v1 (2014).

[4] P.R. Saulson, *Thermal Noise in mechanical experiments*. Phys. Rev. D 42, 2437 (1990).

[5] R. Nawrodt, C. Schwarz, S. Kroker, I. W. Martin, F. Brckner, L. Cunningham, V. Groe, A. Grib, D. Heinert, J. Hough, T. Ksebier, E. B. Kley, R. Neubert, S. Reid, S. Rowan, P. Seidel, M. Thrk, A. Tnnermann, *Investigation of mechanical losses of thin silicon flexures at low temperatures*. Quantum Grav. 30, 115008 (2013).